



ELSEVIER

Physica C 372–376 (2002) 960–962

PHYSICA C

www.elsevier.com/locate/physc

Anisotropic characteristics of the energy dissipation in Bi(2223) ceramics and tapes in weak magnetic fields

Emma Mogilko ^{a,*}, Yakov M. Strel'niker ^{a,b}, Leonid Burlachkov ^{a,c},
Yehuda Schlesinger ^a, Shlomo Havlin ^{a,b}

^a Department of Physics, Bar-Ilan University, Ramat-Gan 52900, Israel

^b Minerva Center, Bar-Ilan University, Ramat-Gan 52900, Israel

^c Institute of Superconductivity, Bar-Ilan University, Ramat-Gan 52900, Israel

Abstract

For practical application of HTSC tapes as current leads, their behavior in realistic conditions, in the presence of magnetic field, becomes crucially important. We have investigated in detail the resistivity transition and the excess resistivity induced by low magnetic fields (1–750 Oe) in highly aligned composite structures of Bi(2223) based tapes and also, for comparison, in bulk ceramics of the same composition. We demonstrate the strong dependence of the electrical and magnetic properties on the microstructure of the composite ceramics. We observed also a dependence of the energy dissipation on the direction of the transport current with respect to the grain orientation. Percolation theory and the effective medium approximation are applied to analyze the anisotropy in the resistive transition of these systems.

© 2002 Elsevier Science B.V. All rights reserved.

Keywords: Bi(2223) tape; Resistive transition; Low magnetic fields; Effective medium approximation

1. Introduction

Practical applications of Bi(2223) based superconducting tapes as electrical leads, depend on their transport properties under realistic conditions, e.g., low magnetic fields are known to reduce drastically the critical current of superconducting coils [1]. It has been also shown [2,3] that the magnetoresistance depends strongly not only on the magnitude of the magnetic field but also on its orientation with respect to the tape surface, increasing sharply with increasing angle. In the present work we investigate the magnetoresistance

of Bi(2223) tapes in weak magnetic fields directed perpendicularly and parallel to the surface of the tape. We compare here the behavior of the superconducting tape in low magnetic fields with that of bulk Bi(2223) ceramics of the same composition. We demonstrate here, that the effective medium approximation (EMA) [4,5] combined with the percolation model provide a consistent fit to the resistive transition in bulk granular HTSC and also in the case of a tape.

2. Experimental

Bi(2223)/Ag tape, 0.15–0.20 mm thick and 0.28–0.3 mm wide was cut into 8.0 mm long strips. The

* Corresponding author. Fax: +972-3-5353298.

E-mail address: mogilko@physnet.ph.biu.ac.il (E. Mogilko).

bulk Bi(2223) ceramic was cut into a $5 \times 4 \times 8$ mm parallelepiped. The microstructure of the cut tape and of the bulk ceramic surfaces perpendicular and parallel to c -axis were investigated by scanning electron microscopy (SEM) and their alignment was checked by XRD. The resistivity was measured by standard four-probe technique using a current density of 5 A/cm^2 for the tapes and 0.5 A/cm^2 for the bulk ceramics. The thermal contact between the sample and the cryostat coldfinger was kept fixed during the measurements at different mutual orientation of the field, current and c -axis. The temperature measurement accuracy was 0.02 K .

3. Experimental results

The tape consists of superconducting filaments (Fig. 1a) built of platelet-like grains with an almost perfect alignment of the superconducting grains ab -planes, parallel to the tape surface, as confirmed by the XRD spectra and as shown here on the SEM image, Fig. 1b.

The bulk, uniaxially compacted, ceramic of the same composition, has a granular structure, each

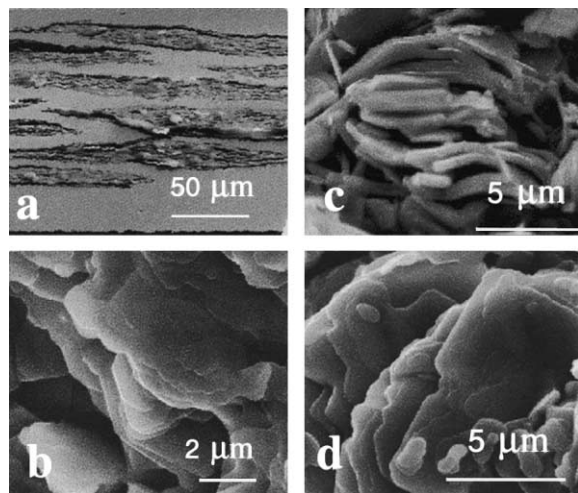


Fig. 1. SEM images of the Bi(2223)/Ag multi-filamentary tape (a,b) and of the Bi(2223) bulk ceramic (c,d). (a) Side view of the tape cross section perpendicular to the filaments. (b) View perpendicular to the tape surface. (c) Side view (along the ab -plane direction) image of the bulk Bi(2223) ceramic. (d) View along the c -axis (direction of the compaction) of the bulk Bi(2223) ceramic.

grain having a platelet-like shape (see Fig. 1c and d). The XRD of the bulk ceramics shows about 85% alignment. The average grain aspect ratio (lateral dimension/thickness) is ~ 60 .

The resistive transition of the tape is quite narrow, about 1 K (see Fig. 2a). Applying low magnetic fields ($\sim 0.1 \text{ mT}$) perpendicular to the tape surface leads to a shift of the resistive transition by $\sim 0.05 \text{ K/G}$ toward lower temperatures (see Fig. 2b). When the field is directed parallel to the tape surface, the shift is much smaller, Fig. 2c.

In the compacted bulk ceramic we observe a shift of $\sim 2.5 \text{ K}$ between the case where the current is parallel to the crystallographic c -axis and the case where the current is parallel to the ab -planes, see Fig. 2d. Applying the field parallel to the grain c -axis, results in a broadening of the lower tail of the resistivity curve, $\rho(T)$, fanning out from the

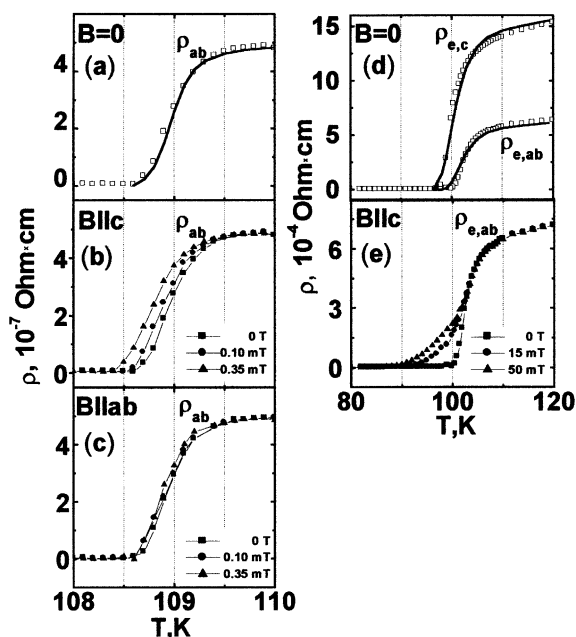


Fig. 2. ρ_c vs T in tape (left) and in bulk Bi(2223) ceramic (right). (a) ρ_c vs T in tape, the open squares are experimental data, the solid line is the theoretical fit based on EMA. (b) The downshift of $\rho_c(T)$ in the tape with increasing magnetic field B , for $B \parallel c$. (c) Same as (b) except $B \parallel ab$. (d) ρ_c vs T in bulk Bi(2223) ceramic; $\rho_{e,c}$ and $\rho_{e,ab}$ (open squares) are the measured resistivities along the c -axis and in the ab -plane, respectively. The solid lines are the theoretical fits based on EMA. (e) $\rho_{e,ab}$ vs T in the bulk ceramic at different fields, $B \parallel c$.

middle of transition. The effect is strongly field dependent, as shown in Fig. 2e.

4. Theory

The structure of the investigated multifilamentary Bi(2223)/Ag tapes is shown in Fig. 1a. The filaments can be approximated by infinitely long, oval cross section, cylindrical inclusions embedded in the homogeneous conducting silver matrix. The volume averaged effective resistivity ρ_e of the tape can be found from the simple relation $1/\rho_e = S_{Ag}/\rho_{Ag} + S_f/\rho_{e,f}$, where S_f is the relative cross section of the filaments (cross section of all filaments/cross section of the tape), S_{Ag} is the similar cross section of the silver matrix (note that $S_f + S_{Ag} = 1$), ρ_{Ag} and $\rho_{e,f}$ are the resistivity of the silver and the volume averaged resistivity of the filaments, respectively.

The conductivity of the individual grains exhibits strong anisotropy: the conductivity along the c -axis is smaller by a factor of $\sim 10^3$ than that in the ab -plane. There is also a strong dispersion of the transition temperature T_c among different grains, i.e., the transition of the sample from normal to superconducting state occurs over some temperature range [6]. This allows us to approximate the granular bulk medium as a mixture of normal and superconducting regions and to use the theories of composite materials and percolating systems. The EMA [4,5] has been applied in the past to high- T_c superconductors [7], mostly for isotropic cases with spherical grains. Although the anisotropic problem can be transformed to the isotropic one by a scaling transformation [8–10] the result will be of a different nature than in the isotropic case. We obtain two coupled self-consistent transcendental equations for the effective volume averaged conductivities in the two perpendicular directions, $\sigma_{e,c}$ (the conductivity along the c -axis) and $\sigma_{e,ab}$ (the conductivity in the ab -plane),

$$p_1 = \frac{\sigma_{1,i} - \sigma_{e,i}}{n_i(\sigma_{1,i} - \sigma_{e,i}) + \sigma_{e,i}} + (1 - p_1) \frac{\sigma_{2,i} - \sigma_{e,i}}{n_i(\sigma_{2,i} - \sigma_{e,i}) + \sigma_{e,i}} = 0$$

where $i = c, ab$; p_1 is the volume fraction of the superconducting part and σ_1, σ_2 are the conductivities of the two constituents. The equations are

coupled via the depolarization factors n_i , which depend both on the shape of the grains as well as on the effective conductivities $\sigma_{e,c}$ and $\sigma_{e,ab}$ [9,10].

The solution of these equations results in the same percolation threshold (i.e., same transition temperature) for the two directions. However, the experimental data show, that the transition to the superconducting state in high- T_c bulk ceramics like Bi(2223) occurs at different temperatures for different directions of the current j : for j parallel to the c -axis it appears at a lower temperature than for j perpendicular to it (Fig. 2d). This can be explained by the presence of the Josephson junctions and their stability with respect to the magnitude of the current. The volume fraction of the superconducting grains depends on the magnitude of the current, and turns out to be different for different directions of j . We have actually two different percolating systems for the two different directions. In the limit $j \rightarrow 0$, both resistivity thresholds tend to the same value.

We find that in order to obtain a good fit to the experimental data, one has to take into account the partial orientational disorder of the single grain crystallographic c -axis. The results of our calculations are in good agreement with experimental data, as can be seen in Fig. 2a and d.

Acknowledgements

This work was supported partly by the US–Israel Binational Science Foundation (BSF) and by the KAMEA fellowship program of the Ministry of Absorption of the State of Israel.

References

- [1] D.C. van der Laan et al., IEEE Trans. Appl. Supercon. 11 (2001) 3345.
- [2] G.C. Han, Phys. Rev. B 52 (1995) 1309.
- [3] G.C. Han, C.K. Ong, Appl. Phys. Lett. 72 (1998) 2751.
- [4] R. Landauer, J. Appl. Phys. 27 (1952) 779.
- [5] D.A.G. Bruggeman, Ann. Phys. (Leipzig) 24 (1935) 636.
- [6] L.I. Glazman et al., Sov. Phys. JETP 67 (1988) 1235.
- [7] D.V. Shantsev et al., Phys. Rev. B 60 (1999) 12485.
- [8] D. Stroud, Phys. Rev. B 12 (1975) 3368.
- [9] Z.D. Genchev, Supercond. Sci. Technol. 6 (1993) 532.
- [10] D.J. Bergman, Y.M. Strelniker, Phys. Rev. B 60 (1999) 13016.